Asian Journal of Chemistry; Vol. 37, No. 4 (2025), 837-842

ASIAN JOURNAL OF CHEMISTRY

https://doi.org/10.14233/ajchem.2025.33447

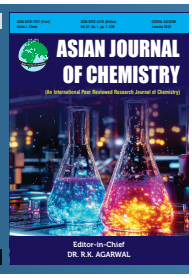

Study of Alumina Supported Calcium Catalyst for Bio-diesel Production using Karanja Oil

ARUN KUMAR GUPTA

Department of Chemical Engineering, School of Engineering and Technology, Chhatrapati Shahu Ji Maharaj University, Kanpur-208024, India

Corresponding author: E-mail: arung247@gmail.com

Received: 30 January 2025; *Accepted*: 27 February 2025; *Published online*: 29 March 2025; AJC-21944

Calcium oxide (CaO) has emerged as an efficient and versatile catalyst for various chemical transformations, particularly in the production of biodiesel and other value-added chemicals. This study highlights the superior catalytic performance of CaO compared to alternative catalysts, demonstrating its ability to deliver higher yields in both methanol and ethanol-based reactions. Its robust stability under reaction conditions ensures prolonged catalytic activity, reducing the need for frequent regeneration. Furthermore, CaO exhibits excellent activity with both methanol and ethanol, exhibiting its adaptability to different feedstocks. The combination of high yield, stability and dual-feedstock activity highlights the potential of CaO as a cost-effective and sustainable catalyst for industrial applications.

Keywords: Karanja oil, Transesterification, CaO, Catalyst, Reusability, Alumina-supported catalyst, Biodiesel production.

INTRODUCTION

The increasing demand for sustainable energy sources has led to a growing interest in biofuels, particularly biodiesel, as an alternative to conventional petroleum-based fuels [1]. Biodiesel, primarily produced through transesterification, offers significant environmental benefits such as reduced greenhouse gas emissions and biodegradability [2]. Among the various feedstocks for biodiesel production, vegetable oils, including Karanja oil, have gained attention due to their high energy content and availability [3]. However, the catalytic process involved in converting these oils into biodiesel requires efficient, cost-effective and eco-friendly catalysts. In recent years, alumina-supported calcium catalysts have emerged as promising candidates for biodiesel production due to their high catalytic activity, stability and ease of synthesis. Calcium, a low cost alkaline earth metal, can effectively promote the transesterification of vegetable oils by breaking the ester bonds and facilitating the conversion into biodiesel [4].

When supported on a material like alumina, which offers a high surface area and enhanced stability, these catalysts exhibit improved performance in terms of reaction efficiency and reusability [5]. This study focuses on the investigation of alumina-supported calcium catalysts for the transesterification of Karanja oil into biodiesel. Karanja oil, derived from the seeds of *Pongamia pinnata* tree, is an under utilized feedstock rich in triglycerides, making it an ideal candidate for biodiesel production. By exploring the synthesis, characterization and catalytic performance of these catalysts, this study aims to contribute valuable insights into the development of more efficient and sustainable biodiesel production processes.

EXPERIMENTAL

Alumina-supported calcium catalyst preparation by incipient impregnation method: The preparation of alumina-supported calcium catalysts using the incipient impregnation method involves the following steps [6]:

(i) Preparation of alumina support: High-purity alumina (AlO_3) as support material was pre-treated by washing with distilled water to remove any impurities or residual moisture. The alumina was then dried at 110 ºC for 12 h to eliminate the excess moisture and ensure the proper surface activation for effective impregnation of calcium precursor.

(ii) Preparation of calcium precursor solution: A solution of the desired concentration was prepared by dissolving calcium acetate salt in distilled water [7]. The concentration of calcium precursor was selected according to the desired calcium loading on the alumina support. The solution was agitated to ensure homogeneous dissolution of the salt.

(iii) Impregnation process: The dried alumina substrate was subsequently impregnated with the calcium precursor solution using the impregnation technique [6]. During this procedure, the alumina was placed in a beaker and the calcium solution was gradually introduced, ensuring complete wetting of the alumina's pore structure without the presence of excess liquid. The alumina is allowed to absorb the solution for an adequate duration (typically 1 to 2 h), ensuring that the entire surface of alumina was saturated with the calcium precursor.

(iv) Drying and calcination: After the impregnation, the catalyst precursor was dried at 110 ºC for 12 h to remove the remaining water and solvents from the impregnated solution. The dried material was then subjected to calcination in a muffle furnace at different temperature of 700-500 ºC for 4 h. This step promotes the thermal decomposition of calcium salt, resulting in the formation of calcium oxide (CaO) supported on the alumina surface. The calcination process also helps to enhance the stability and dispersion of calcium on the alumina support [8].

(v) Cooling and final catalyst: After calcination, the catalyst was allowed to cool to room temperature in a desiccator to prevent moisture absorption. The final alumina-supported calcium catalyst was characterized and use in biodiesel production.

Catalyst characterization: The surface area of the catalyst samples were measured using nitrogen adsorption at 77 K in a SMART SORBS 92/93 set up. The single point BET equation was used to calculate the surface area. The XRD patterns of the supported samples were obtained with a 180 Debye Flex-2002 X-ray diffractometer. Nickel filtered $K\alpha$ radiation of a copper target ($\lambda = 1.541841$ Å) was employed and the data was obtained from 20º to 70º in a step mode at a 2θ sweep of 3º min^{-1} and a time constant of 3 s. The UV-vis spectra were obtained using a Cary 5000 UV-vis-NIR spectrophotometer equipped with a Harrick Scientific diffuse reflectance accessory. All spectra were collected under ambient conditions with $BaSO_4$.

Reactor used: A 2.0 L batch reactor (AmAr Equipments Ltd, Mumbai, India) was used for most of the transesterification experiments [9]. The reactor was equipped with a PID controller, a RTD-PT100 temperature sensor, an electrically heated jacket, a condenser with a cooling water circulation system, an agitator for proper mixing, a valve for sample removal and gauges. The same batch reactor was previously used for biodiesel production. Bench top experiments were also performed in an agitated 250 mL beaker with proper temperature control. The bench top experiments were performed for the exploratory studies.

Experimental procedure: Known amounts of methanol and 3.5% g/g-oil liquid-phase catalysts, were thoroughly mixed at room temperature. This solution was then added to the bottom of batch reactor or beaker depending on the type of study. In the beaker experiments, 100 g of soybean oil was added and the temperature was then raised to 333 K. The reaction was allowed to continue for 1 h after and then biodiesel yield was determined. In 2 L batch reactor, 250 g of soybean oil was added and then the transesterification reaction using solid-phase catalysts were carried out from 293 K to 333 K. At each temperature, a fresh stock of reactant and solid catalyst was considered. The required amount of supported catalyst and volume of methanol, with methanol to oil molar ratios of 3:1, 6:1, 12:1 or 24:1, were added to the reactor. To calculate the molar ratio, the molecular weight of soybean oil was taken to be 882.82 g/mol. A previous study reported a molecular weight of soybean oil as 874 g/mol [10]. Samples (about 20 mL) were withdrawn at various time-intervals for biodiesel yield determination. The extracted samples were permitted to settle for 12 h, agitated and then rinsed with distilled water at 343 K, targeting the upper biodiesel layer. The upper ester layer of the samples were analyzed with NMR spectroscopy for the calculation of yield using previously established procedures [11]. Several runs were repeated to check for reproducibility and the average value was reported.

Catalyst leaching: To study the effect of catalyst leaching, the following procedure was followed. The powder form of Al_2O_3 supported Na catalyst was mixed with the amount of methanol required for the reaction. The amount of methanol required was according to the methanol to oil ratio. The solid-phase was then separated from the liquid phase by decantation and then by filtration. The liquid phase containing methanol and any leached material was then taken in the beaker or batch reactor specified above. A known amount of oil corresponding to the methanol to oil was then mixed with the liquid phase mixture and the reaction was carried out under the appropriate operating conditions based on the specific study [12].

RESULTS AND DISCUSSION

Calcium loading effect: As the calcium loading increases from 5% to 20%, the absorption in the NIR region becomes more intense and sharper (Fig. 1). This indicates the increased presence of calcium oxide species and their interactions with the alumina support. At lower loadings (5% and 10%), the calcium species are better dispersed on the alumina surface, leading to weaker absorption features. As the loading increases (15% and 20%), calcium aggregation occurs and the absorption

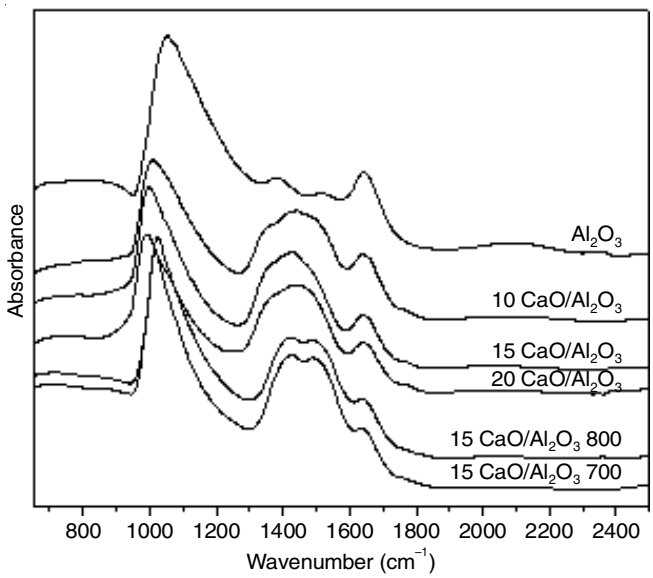

Fig. 1. UV graph of CaO/Al_2O_3 of different loading

becomes more pronounced due to the formation of larger CaO particles and clusters.

Surface hydroxyl groups: Absorption bands in the range of 1000-1400 nm are often associated with the presence of surface hydroxyl groups, which can interact with CaO [13]. These bands may shift or increase in intensity as the calcium loading increases, reflecting the increased availability of active sites and changes in the surface structure.

Bonding and aggregation: The intensity and position of the peaks in the 1400-2000 nm range are indicative of Ca-O bonding. At higher calcium loadings, aggregation of calcium oxide is observed, which leads to a more crystalline structure and stronger bonding interactions with the alumina support.

Effect of methanol and ethanol in biodiesel production process: The effect of methanol and ethanol on biodiesel conversion was investigated using different alcohol-to-oil ratios of 6:1, 12:1, 15:1 and 30:1. Methanol consistently showed better conversion rates compared to ethanol across all ratios. At a 6:1 methanol-to-oil ratio, the conversion achieved was 17%, whereas ethanol produced only 2% conversion. However, at a 12:1 ratio, methanol exhibited a significant increase in conversion to 98%, demonstrating its superior reactivity in the transesterification process. In contrast, ethanol showed a modest improvement, reaching 17% conversion at the same ratio. At higher methanol-to-oil ratios of 15:1 and 30:1, the conversion dropped dramatically for methanol, with the conversion falling to 4% and 0%, respectively as shown in Fig. 2. Ethanol also experienced a decline in conversion with increasing alcohol-to-oil ratios, but to a lesser extent, showing 63% conversion at 15:1 and 5% conversion at 30:1. These results suggest that while methanol is more efficient than ethanol, excessive amounts of alcohol in the reaction mixture can negatively impact the conversion efficiency. The diminishing returns at higher alcohol-to-oil ratios for both methanol and ethanol can be attributed to factors such as excess alcohol interfering with phase separation, reduced catalyst efficiency and the equilibrium constraints of the transesterification reaction [14].

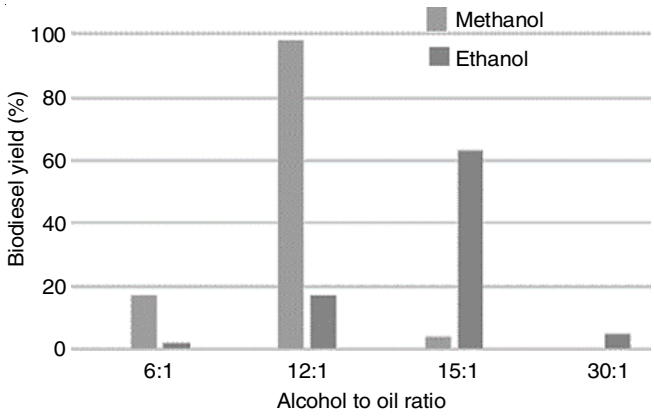

Fig. 2. Biodiesel yield at different alcohol to oil ratio

Methanol activated calcium oxide catalyst: The increase in conversion from 17% to 30% when using methanol-activated calcium oxide (CaO) as catalyst can be attributed to several key factors that enhance the catalytic activity of CaO. When methanol was introduced into the system, it activates the CaO catalyst by promoting the formation of more reactive species on the catalyst surface. Methanol, as a polar solvent, enhances the dissolution of oil and facilitates the dispersion of catalyst particles, thereby increasing the surface area available for the reaction. Herein, methanol may facilitate the generation of more hydroxyl groups (OH^-) on the surface of CaO, which act as active sites for the transesterification process, improving the reactivity of catalyst.

Moreover, methanol can also help in the deactivation of CaO by breaking any surface carbonate bonds that might form during the reaction, leading to the regeneration of active sites. As a result, methanol activation increases the efficiency of CaO catalyst by providing more reactive sites for the esterification reaction. The enhanced solubility and better phase mixing of the reactants due to methanol also help in improving the conversion rate. Therefore, the methanol-activated CaO catalyst shows a higher conversion of oil to biodiesel, as it effectively facilitates the transesterification reaction by increasing the number of accessible active sites and improving the reaction conditions.

Leaching effect on CaO catalyst: In case of CaO used as a catalyst for biodiesel production, no leaching of calcium ions into the reaction medium was observed. Leaching refers to the loss of catalyst components into the product mixture during the reaction, which could significantly reduce the catalytic efficiency and cause contamination of biodiesel [15]. However, in this study, the CaO catalyst demonstrated excellent stability and durability throughout the reaction process. The CaO remained intact in its solid phase, without any detectable calcium ion release into the oil-methanol mixture. This is attributed to the high stability of CaO under the conditions used in the transesterification process as well as its strong ionic bond structure, which prevents the migration of calcium ions. The non-leaching behaviour of catalyst ensures that it remains an effective and reusable catalyst for biodiesel production, reducing the requirement for the frequent catalyst replacement and minimizing the risk of contamination in biodiesel product as shown in Fig. 3.

The UV spectra of both fresh and used catalysts confirmed that no leaching of CaO catalyst during the reaction was observed. No significant changes in the absorption peaks were observed before and after the reaction, indicating that CaO catalyst remained stable and did not dissolve or release any metal species into the reaction medium [16]. This stability suggests that the catalyst effectively maintained its structural integrity and catalytic activity throughout the process, without any undesirable loss of material or performance degradation due to leaching.

Effect of methanol to oil ratio and THF as co-solvent: The presence of CaO in the alumina-supported calcium catalyst plays a crucial role in enhancing the transesterification reaction during biodiesel production. One of the key factors influencing the conversion rate of oils into biodiesel is the methanol-to-oil ratio. As the amount of methanol is increased in the reaction mixture, the conversion efficiency improves significantly as shown in Fig. 4. Calcium oxide facilitates the breaking of ester bonds in the triglycerides of oils, promoting the formation of methyl esters (biodiesel). When the methanol-to-oil ratio incre-

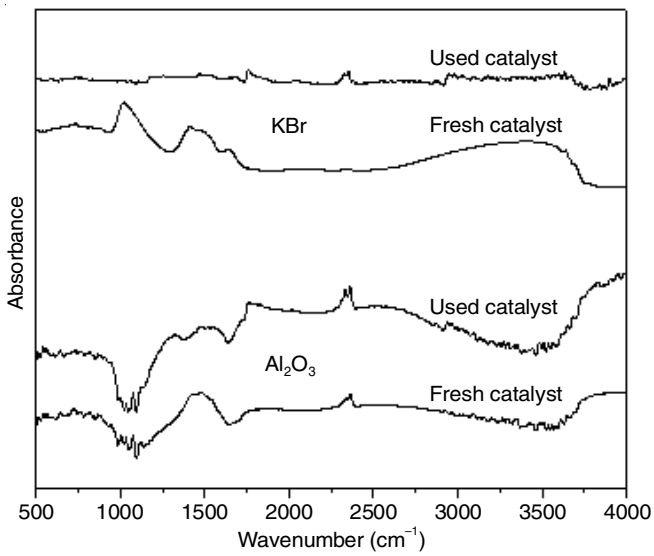

Fig. 3. UV spectra of fresh and used catalyst for leaching effect

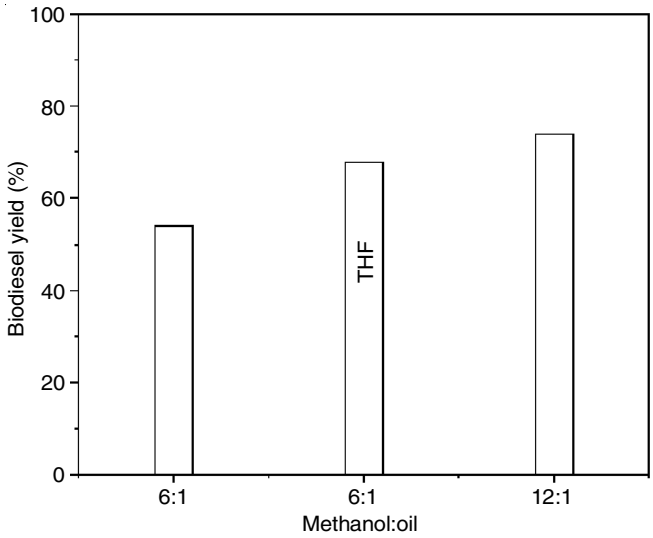

Fig. 4. Effect of methanol to oil ratio and THF as co-solvent

ased, the availability of methanol molecules enhances the reaction kinetics, allowing for a more complete transesterification process. In presence of CaO, which acts as a basic catalyst, the increased methanol concentration accelerates the formation of biodiesel by shifting the equilibrium towards ester production. This leads to a higher conversion rate, as excess methanol helps in overcoming any potential equilibrium limitations, driving the reaction to completion. Therefore, a higher methanol-to-oil ratio, in combination with CaO, results in a more efficient and higher-yield biodiesel production process.

The use of tetrahydrofuran (THF) as a co-solvent in the transesterification process significantly enhances biodiesel production yields [17]. THF, being a polar aprotic solvent, improves the solubility of both oil and methanol, which are otherwise immiscible to some extent. This increased solubility facilitates a more efficient interaction between the methanol and the oil, allowing for a smoother and faster transesterification reaction. By acting as a co-solvent, THF helps in breaking the viscosity of vegetable oils, promoting better dispersion of the catalyst and methanol throughout the oil phase. Moreover, THF helps to reduce the formation of emulsions that might hinder the separation of biodiesel from glycerol, further improving the purity and yield of the biodiesel. As a result, the presence of THF in the reaction mixture increases the overall biodiesel production yield, improves reaction kinetics and ensures a more efficient and complete conversion of triglycerides into biodiesel.

Catalyst reusability stability: In the biodiesel production process using a 12:1 methanol-to-oil ratio and calcium oxide (CaO) as catalyst with 3.5% loading, the catalyst demonstrated significant catalytic activity in the first run, achieving a high conversion rate of 98%. However, upon reuse of CaO catalyst for subsequent runs, a significant decline in conversion efficiency was observed. After the second run, the conversion decrease sharply to 58%, indicating a decrease in the effectiveness of catalyst. This reduction in the catalytic performance continued in the third run, where the conversion decreased further to 4% and in the fourth run, the conversion was almost negligible, at 0%. The observed decrease in conversion after each reuse suggests that the CaO catalyst underwent deactivation over time as shown in Fig. 5. This deactivation could be attributed to factors such as catalyst poisoning, sintering or leaching of calcium material, which affected the surface area and active sites of catalyst [18].

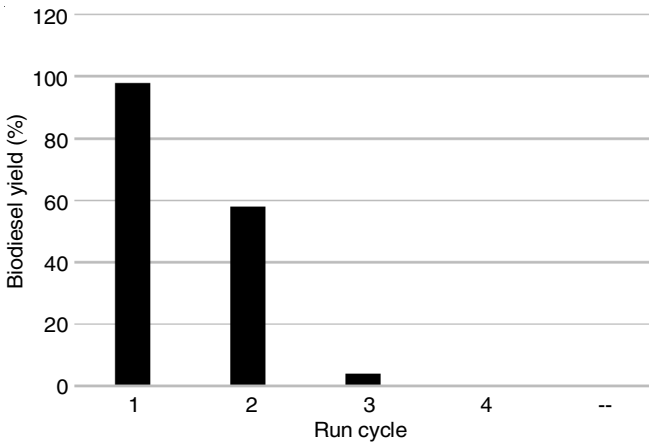

Fig. 5. Reusability test of the CaO catalyst

The used CaO catalyst, even after multiple catalytic cycles, exhibited identical UV spectra to both the fresh and regenerated catalysts, demonstrating remarkable stability and consistency in its catalytic properties. No significant shifts or changes in the characteristic peaks, indicating that the CaO catalyst retained its structural integrity and functionality after repeated use and regeneration [19]. This suggests that the catalyst did not undergo significant deactivation or alteration of its surface structure during the reaction cycles and able to effectively recover its activity upon regeneration. The consistent UV spectral profile, both for the fresh and used catalyst, underscores the long-term stability and durability of the CaO catalyst, making it a reliable choice for processes requiring multiple catalytic cycles.

Storage stability of CaO catalyst: The CaO catalyst shows remarkable stability even after prolonged storage (6 month),

as evidenced by the UV spectra analysis. UV spectra shown more noise regardless of moisture. Both the fresh and stored samples exhibited similar absorption patterns as shown in Figs. 6 and 7, confirming that the catalyst does not undergo significant structural or chemical changes over time. This indicates that the CaO catalyst retains its integrity and catalytic properties, even after being stored for extended periods. The absence of any significant shifts or peaks in the UV spectra further supports the conclusion that the catalyst remains stable, ensuring reliable performance in the catalytic processes even after long-term storage.

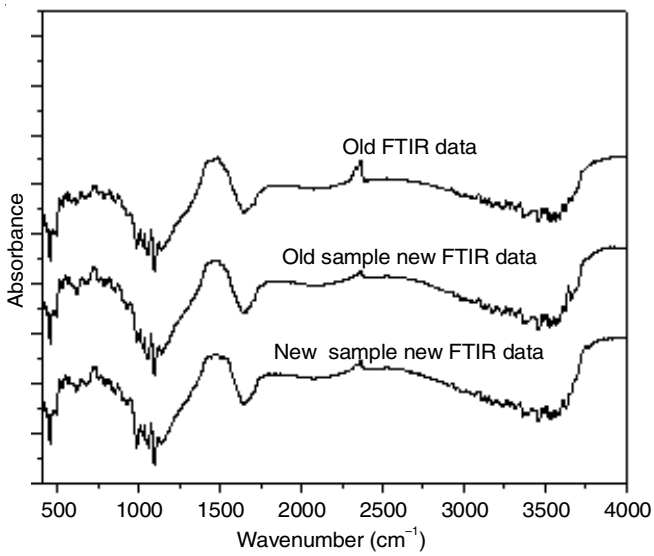

Fig. 6. UV spectra of CaO catalyst for different storage time without calcined sample

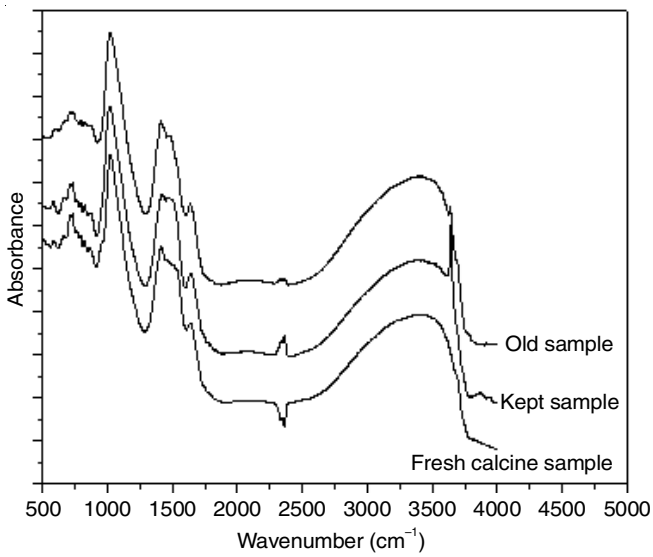

Fig. 7. UV spectra of CaO catalyst for different storage time with calcined sample

Effect of calcination temperature on catalyst structure: CaO exhibits similar UV spectra when calcinated at different temperatures due to the retention of its fundamental electronic structure and optical properties. During calcination, $CaCO_3$ decomposes to form CaO and the process predominantly removes volatile components like CO without significantly altering the electronic transitions responsible for UV absorption [19]. Consequently, the UV spectra remain consistent as shown in Fig. 8, as these transitions are governed by the intrinsic electronic configuration of CaO, which does not vary significantly with temperature changes within the calcination range. Minor variations, if any, may result from surface defects or impurities introduced during the process.

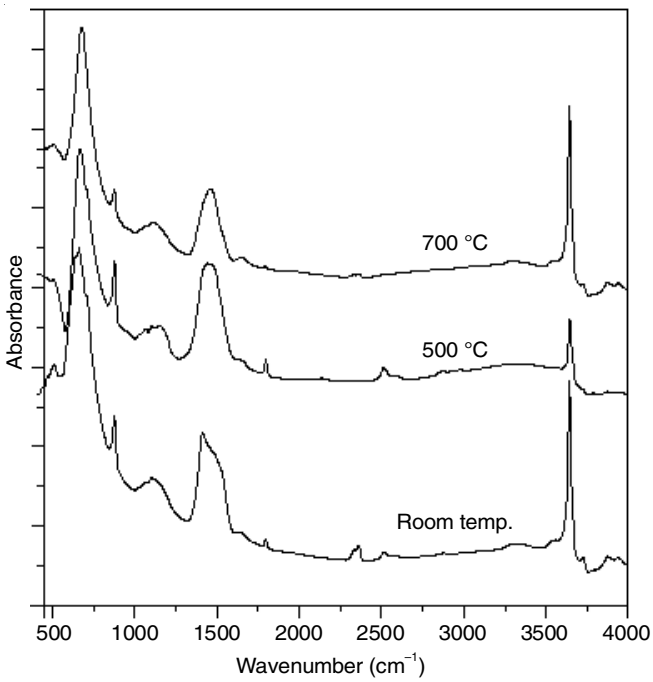

Fig. 8. UV spectra of different calcination temperature

The UV spectra of CaO catalyst reveal distinct carbonate (CO_3^{2-}) peaks in the range of 1750-1250 cm^{-1}, which are characteristic of surface-bound carbonate species. These peaks are typically associated with the interaction of CaO with carbon dioxide or moisture, leading to the formation of carbonate groups on the catalyst surface as shown in Fig. 9. The presence of these CO_3 peaks suggests that the CaO catalyst undergoes surface carbonation, a common phenomenon for basic metal oxides like calcium oxide. The intensity and position of these peaks can also provide insights into the extent of carbonation, which can influence the catalytic properties of CaO, particularly in reactions involving CO or other carbon-containing species.

Effect calcium acetate as precursor: The CaO catalyst, derived from calcium acetate as precursor and calcined at different temperatures (500, 600 and 700 ºC), exhibited consistent catalyst stability across the different calcination conditions [20]. UV spectra (Fig. 10) confirmed that calcium acetate as a precursor forms a stable CaO phase and does not significantly degrade or lose its catalytic properties with varied calcinied temperature. The similar UV spectral features, including the behaviour of characteristic carbonate and hydroxyl peaks, further support the conclusion that the catalyst maintains its effectiveness and stability even after calcination at higher temperatures, ensuring reliable performance in the catalytic applications.

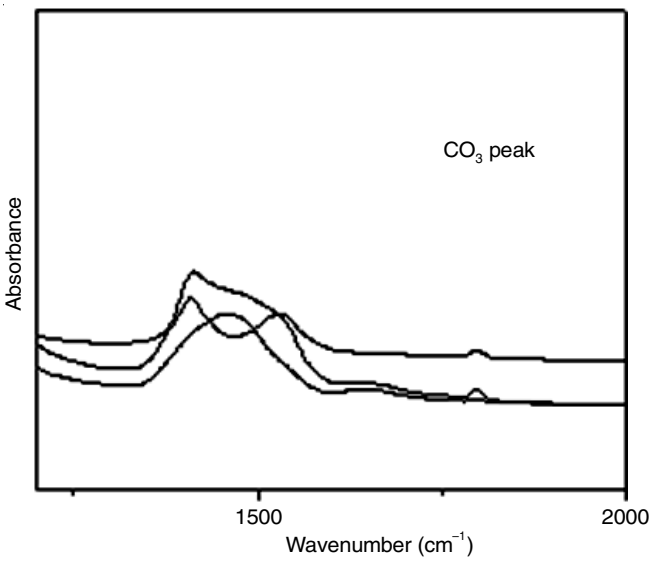

Fig. 9. Presence of carbonate peak in UV spectra

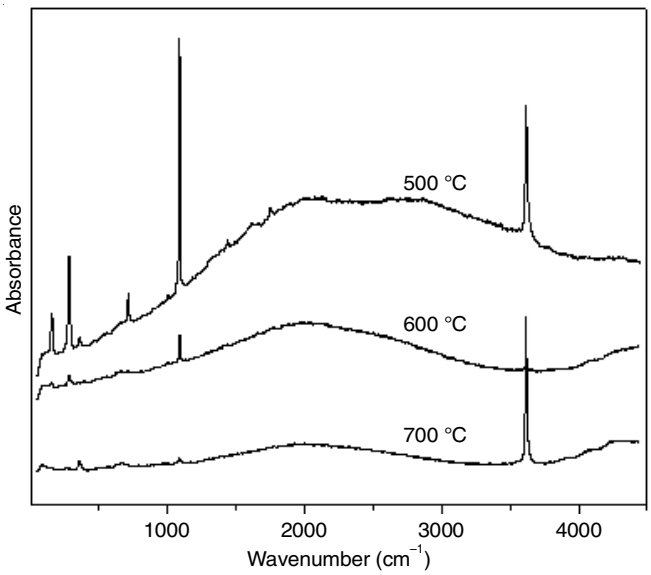

Fig. 10. UV spectra CaO obtained from calcium acetate as the precursor and calcined at various temperatures

Conclusion

In conclusion, the alumina-supported calcium catalyst demonstrates significant potential for biodiesel production from Karanja oil. The high surface area and alkaline nature make it an effective choice for transesterification reactions, facilitating the conversion of Karanja oil into biodiesel with good yield and efficiency. The study highlights the advantages of using locally available materials, such as alumina and calcium, for biodiesel production, offering a sustainable, cost-effective solution to address the rising demand for renewable energy sources. Furthermore, the stability and reusability of the catalyst enhance its practical applicability, providing a promising pathway for large-scale biodiesel production. Future work could focus on optimizing the catalyst preparation process, enhancing its catalytic activity and exploring its performance in various reaction conditions to further improve biodiesel yields and lower production costs.

CONFLICT OF INTEREST

The authors declare that there is no conflict of interests regarding the publication of this article.

REFERENCES

1. D. Huang, H. Zhou and L. Lin, *Energy Procedia*, **16**, 1874 (2012); https://doi.org/10.1016/j.egypro.2012.01.287
2. S.M. Farouk, A.M. Tayeb, S.M.S. Abdel-Hamid and R.M. Osman, *Environ. Sci. Pollut. Res. Int.*, **31**, 12722 (2024); https://doi.org/10.1007/s11356-024-32027-4
3. R.L. Patel and C.D. Sankhavara, *Renew. Sustain. Energy Rev.*, **71**, 464 (2017); https://doi.org/10.1016/j.rser.2016.12.075
4. R. Abd Rabu, I. Janajreh and D. Honnery, *Energy Convers. Manage.*, **65**, 764 (2013); https://doi.org/10.1016/j.enconman.2012.02.031
5. W.N.R.W. Isahak and A. Al-Amiery, *Green Technol. Sustainab.*, **2**, 100078 (2024); https://doi.org/10.1016/j.grets.2024.100078
6. B.A.T. Mehrabadi, S. Eskandari, U. Khan, R.D. White and J.R. Regalbuto, *Adv. Catal.*, **61**, 1 (2017); https://doi.org/10.1016/bs.acat.2017.10.001
7. C.N. Fredd and H.S. Fogler, *Chem. Eng. Sci.*, **53**, 3863 (1998); https://doi.org/10.1016/S0009-2509(98)00192-4
8. R. Khalil, K. Rusli and Andri, *World Vet. J.*, **11**, 578 (2021); https://doi.org/10.54203/scil.2021.wvj73
9. A.K. Gupta, *J. Indian Chem. Soc.*, **100**, 100970 (2023); https://doi.org/10.1016/j.jics.2023.100970
10. W. Xie and L. Zhao, *Fuel*, **103**, 1106 (2013); https://doi.org/10.1016/j.fuel.2012.08.031
11. M.D. Guillen and A. Ruiz, *Trends Food Sci. Technol.*, **12**, 328 (2001); https://doi.org/10.1016/S0924-2244(01)00101-7
12. J.M. Marchetti, V.U. Miguel and A.F. Errazu, *Renew Sustain. Energy Rev.*, **11**, 1300 (2007); https://doi.org/10.1016/j.rser.2005.08.006
13. O. Humbach, H. Fabian, U. Grzesik, U. Haken and W. Heitmann, *J. Non-Cryst. Solids*, **203**, 19 (1996); https://doi.org/10.1016/0022-3093(96)00329-8
14. I.A. Musa, *Egyptian J. Petroleum*, **25**, 21 (2016); https://doi.org/10.1016/j.ejpe.2015.06.007
15. A.J. Martín, S. Mitchell, C. Mondelli, S. Jaydev and J. Pérez-Ramírez, *Nat. Catal.*, **5**, 854 (2022); https://doi.org/10.1038/s41929-022-00842-y
16. W. Mäntele and E. Deniz, *Spectrochim. Acta A Mol. Biomol. Spectrosc.*, **173**, 965 (2017); https://doi.org/10.1016/j.saa.2016.09.037
17. I. Ridwan, H. Budiastuti, R. Indarti, N.L.E. Wahyuni, H.M. Safitri and R.L. Ramadhan, *Mater. Sci. Energy Technol.*, **6**, 15 (2023); https://doi.org/10.1016/j.mset.2022.11.002
18. P. Forzatti and L. Lietti, *Catal. Today*, **52**, 165 (1999); https://doi.org/10.1016/S0920-5861(99)00074-7
19. A. Scaltsoyiannes and A. Lemonidou, *Chem. Eng. Sci. X*, **8**, 100071 (2020); https://doi.org/10.1016/j.cesx.2020.100071
20. S.F. Basumatary, S. Brahma, M. Hoque, B.K. Das, M. Selvaraj, S. Brahma and S. Basumatary, *Green Energy Resour.*, **1**, 100032 (2023); https://doi.org/10.1016/j.gerr.2023.100032